Journal of
Babol University of Medical Sciences
JBUMS
e-ISSN: 2251-7170 p-ISSN: 1561-4107

Evaluation of Submandibular Gland Fossa Concavity Using Cone-Beam Computed Tomography

S. H. Razavi (DDS, MS)[1], A. Ansarilari (DDS, MS)[*1], M. Poormohammadi (DDS, MS)[1]

1.Department of Oral and Maxillofacial Radiology, School of Dentistry, Shahid Sadoughi University of Medical Sciences, Yazd, I.R.Iran.

•**Corresponding Author: A. Ansarilari (DDS, MS)**
Address: School of Dentistry, Shahid Sadoughi University of Medical Sciences, Imam Reza Boulevard, Yazd, I.R.Iran.
Tel: +98 (35) 36256975. **E-mail:** ansari.1376@gmail.com

Article Type
Research Paper

Received:
Nov 18th 2024
Revised:
Dec 30th 2024
Accepted:
Jan 19th 2025

ABSTRACT

Background and Objective: The submandibular gland fossa is one of the most critical anatomical regions in implant therapy of the posterior mandible. The present study was conducted to evaluate the location and anatomical characteristics of this fossa using cone-beam computed tomography (CBCT).

Methods: In this cross-sectional study, 140 CBCT images were selected from the archives of the Radiology Department of Yazd School of Dentistry, and the frequency of deep submandibular gland fossa was evaluated. In cases with a U-shaped ridge, the location, depth, angle of concavity, and distance from the deepest point of the fossa to the alveolar crest were calculated according to sex (male/female) and side (left/right).

Findings: The frequency of deep submandibular gland fossa (U-shaped ridge) was 56.4%. The mean concavity depth in men (2.86±0.70 mm) was significantly greater than in women (2.42±0.57 mm) ($p<0.001$). This value was also significantly greater on the right side (2.67±0.60 mm) compared to the left side (2.45±0.68 mm) ($p<0.05$). The distance from the deepest point of the submandibular gland fossa to the alveolar crest was also significantly greater in men (15.34±2.31 mm) compared to women (13.33±2.10 mm) ($p<0.001$). The overall mean concavity angle in the study population was 42.76±7.91 degrees. The location of the deepest point of the fossa in men (aligned with the distal half of the second mandibular molar) was significantly different from and more posterior than that in women (aligned with the junction between the first and second mandibular molars) ($p<0.05$).

Conclusion: The results of the study demonstrated that the frequency of the submandibular gland fossa in the studied population is high. Therefore, thorough evaluation of this region on CBCT imaging prior to implant treatment in the mandibular molar areas is essential.

Keywords: *The Submandibular Gland Fossa, Cone-Beam Computed Tomography (CBCT), Dental Implants, Anatomy.*

Cite this article: Razavi SH, Ansarilari A, Poormohammadi M. Evaluation of Submandibular Gland Fossa Concavity Using Cone-Beam Computed Tomography. *Journal of Babol University of Medical Sciences*. 2026; 28: e12.

Introduction

Today, the use of dental implants is fundamental in the management of edentulous areas. Dental implants require proper osseointegration to achieve maximum comfort and aesthetics, which is only possible when the implant is positioned in the correct location. Treatment failure may occur due to improper implant placement, resulting in bone perforation, inflammation, infection, or even mandibular fracture. The most critical anatomical regions are the posterior mandible, the inferior alveolar nerve, and the submandibular gland fossa, as the submental and sublingual arteries pass through this region (1).

Dental implant surgery may be associated with complications such as bleeding, infection, sinus issues, nerve injuries, improper placement, mandibular fracture, damage to the salivary glands, loosening of the tooth adjacent to the implant, airway obstruction, and aspiration (2-4). The causes of these complications may include poor treatment techniques, lack of effective communication between dental specialties, and insufficient time devoted to preoperative planning, such as radiographic evaluation and measurements and preparation of an appropriate surgical guide. Of course, knowledge of anatomy should not be overlooked either (4).

The submandibular gland fossa is a concavity on the internal, posterior-inferior surface of the mandible that extends to the mylohyoid ridge, and it houses the submandibular salivary gland. Perforation of this area can lead to life-threatening consequences due to bleeding and hematoma formation (1, 5). Knowledge of the depth of this fossa prior to implant placement in the posterior mandible is essential, especially when it is deep; if not recognized, it may result in perforation of the lingual plate (6). This condition is an adverse outcome that can cause inflammation and infection, subsequently leading to implant loss. If the perforation site is located above the mylohyoid ridge, it may cause paresthesia of the lingual nerve; if located below this area, it may result in injury to the inferior alveolar nerve (7, 8).

In order to assess ridge concavity and select the appropriate implant fixture size, obtaining a suitable radiograph as a guide for the surgeon is highly critical. Helical CT can provide this information; however, CBCT is a better choice due to its lower cost, significantly lower radiation dose, and higher resolution (8). The American Academy of Oral and Maxillofacial Radiology states that CBCT cross-sectional images are essential prior to implant placement. These images are helpful in accurately determining the size, angle, and location before and after implant placement (9-11).

Given the importance of understanding the anatomical variations of the submandibular gland fossa in the posterior mandible for the success of implant treatment (7), this study was conducted to evaluate the location of the deepest point, its distance from the alveolar crest, the buccolingual dimension, and the degree of concavity of the submandibular gland fossa in the first and second molar regions, comparing the left and right sides of the mandible in regard to sex, and using CBCT in patients referred to the Yazd School of Dentistry.

Methods

This cross-sectional study was conducted after approval by the Ethics Committee of Shahid Sadoughi University of Medical Sciences in Yazd with the code IR.SSU.DENTISTRY.REC.1402.017. A total of 140 files were selected from the CBCT archive images of patients who had referred to the Department of Oral and Maxillofacial Radiology at Yazd School of Dentistry during the years 2023-2024. The selection was based on study inclusion criteria. The inclusion criteria were: age of 18 to 65 years, presence of bilateral permanent mandibular first and second molars in the image, no history of trauma, surgery, or any pathology in the image, and images of good quality with no patient movement artifacts.

The images were acquired using a Planmeca ProMax 3D Mid imaging unit (Helsinki, Finland), with a field of view of 20×17 cm and a voxel size of 100 μm. The exposure parameters were set at 90 kVp, a current of 8 mA, and an exposure time of 15 seconds for the images. The images were initially saved in DICOM format. The data were assessed in Romexis software. After adjusting the appropriate head position so that the occlusal surface of the molar teeth was parallel to the horizontal line, a panoramic curve was reconstructed using the axial view, and the path of the inferior alveolar nerve canal was identified. Cross-sectional images were generated at the location of the mandibular first and second molars. The thickness of each slice and the interval between them were set by default to 2 mm. According to a study by Chan et al. (12), the ridge morphology of patients was classified into three groups: C-shape, P-shape, and U-shape. In a C-shaped ridge, the base of the ridge is wider than its crest; in a U-shaped ridge, the ridge crest is wider than its base; and in a P-shaped ridge, the crest and base have similar buccolingual widths. In the U-shaped group, which included patients with a deep submandibular gland fossa (12), the deepest point of the submandibular gland fossa was determined by comparing measurements on cross-sectional views and designated as point "A". The location of the deepest point was classified as I through VII as follows: I: deepest point in the mesial half of the first molar, II: deepest point in the middle portion of the first molar, III: deepest point in the distal half of the first molar, IV: deepest point between the first and second molars, V: deepest point in the mesial half of the second molar, VI: deepest point in the middle portion of the second molar, VII: deepest point in the distal half of the second molar (Figure 1).

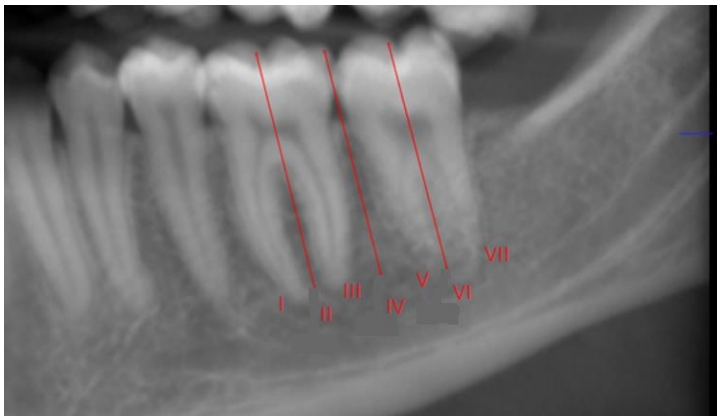

Figure 1. Classification of the depth of the submandibular gland fossa

The depth and angle of the concavity were also calculated in this region. This was performed as follows: a line was drawn connecting the most prominent superior and inferior points of the concavity. From this line, a perpendicular line was extended to the deepest point of the fossa, and the length of this perpendicular was recorded as the fossa depth. Subsequently, a horizontal line was drawn from the deepest point of the fossa (point A), designated as line "B." The angle between this line and the line connecting the most prominent superior point of the concavity to point "A" (line C) determined the angle of the concavity (α) (Figure 2). The available bone height was also measured from the deepest point of the concavity to the alveolar crest, along a line parallel to the longitudinal axis of the tooth (Figure 3). These measurements were similarly performed on the contralateral side for comparison. All measurements were conducted by a single qualified examiner.

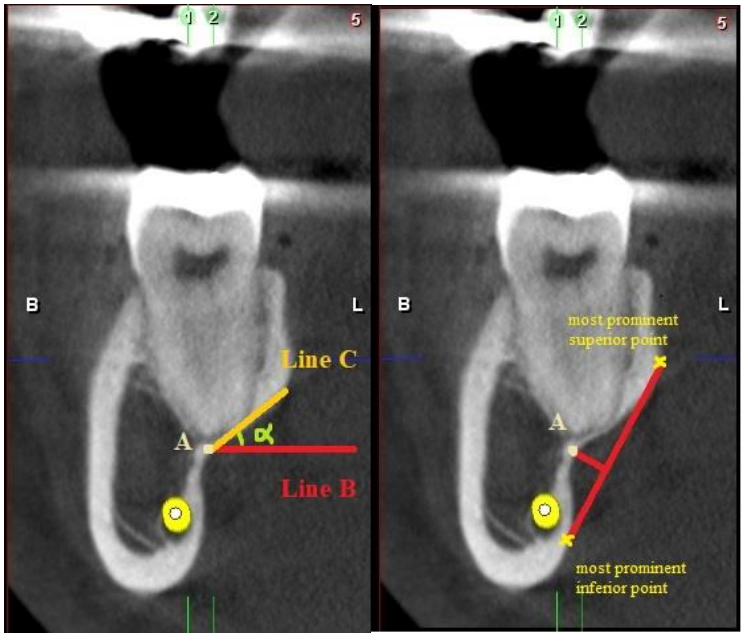

Figure 2. Measurement of the depth and degree of concavity

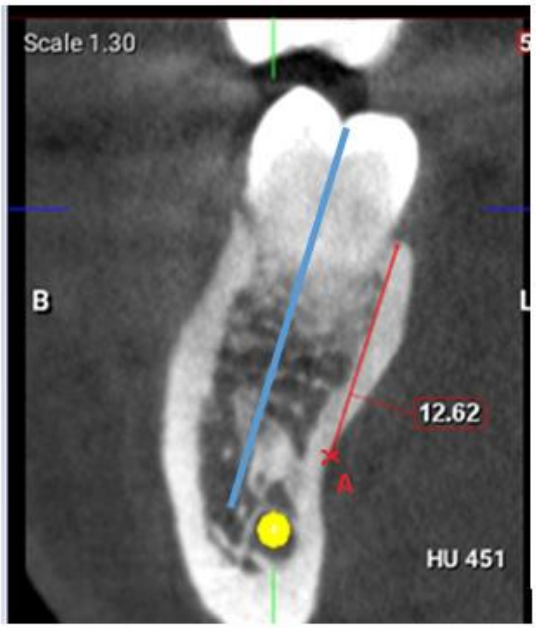

Figure 3. Vertical distance from the deepest point (A) to the alveolar crest. (The blue line represents the longitudinal axis of the tooth

After collecting data, they were entered into SPSS software version 27. The normality of quantitative data was assessed using the Kolmogorov–Smirnov test. Given the normal distribution of the data, Chi-square test, Fisher's exact test, and independent sample t-test were employed for data analysis. A p-value<0.05 was considered statistically significant.

Results

Of the 140 CBCT images examined, 101 belonged to females (72.1%) and 39 to males (27.9%). The mean age of the participants was 31.03±9.46 years (range: 18-64 years). Based on the ridge morphology classification on CBCT, 79 patients (56.4%) exhibited a U-shaped ridge, 14 patients (10%) a C-shaped ridge, and 47 patients (33.6%) a P-shaped ridge. When classified by sex, the most common ridge morphology in both females and males was the U-shape, while the least common was the C-shape; however, no statistically significant difference was observed between males and females regarding posterior mandibular ridge morphology. Furthermore, ridge morphology was identical on both sides; therefore, it was not included in the statistical analysis. Subsequent statistical analyses were performed on the 79 samples exhibiting U-shaped morphology.

The highest frequency of U-shaped ridge morphology by sex was observed in females (68.4%). Regarding the location of the deepest point of the submandibular gland fossa in relation to adjacent teeth in males, the highest frequency was at site VII (26%) and the lowest frequency at site I (2%). In females, the highest frequency of the deepest point location was at site IV (28.7%) and the lowest frequency at site I (2.8%). A statistically significant difference was observed between males and females regarding the frequency distribution of the deepest point location of the submandibular gland fossa (p=0.031).

The highest frequency of the deepest point location of the submandibular gland fossa relative to the teeth on the right side was at site IV (31.6%), and the lowest frequency was at site I (2.5%). On the left side, the highest frequency was at site V (29.1%), and the lowest frequency was at site I (2.5%). No statistically significant difference was found in the frequency distribution of the deepest point location relative to the teeth between the two sides.

Although the mean concavity angle (concavity degree) of the submandibular gland fossa was greater in females than in males, this difference was not statistically significant (Table 1). The mean depth of the submandibular gland fossa concavity and the mean distance from the deepest point of the fossa to the alveolar crest along the longitudinal axis of the tooth were significantly greater in males compared to females (Table 1).

Table 1. Comparison of mean concavity angle, depth, and distance from the deepest point of the fossa to the alveolar crest by sex

Variable	Male (n=50) Mean±SD	Female (n=108) Mean±SD	Total Mean±SD	p-value
Angle (degrees)	42.22±8.43	43.01±7.68	42.76±7.91	0.561
Depth (mm)	2.86±0.70	2.42±0.57	2.56±0.65	<0.001
Distance (mm)	15.34±2.31	13.33±2.10	13.96±2.36	<0.001

There was no statistically significant difference between the right and left sides regarding the mean concavity angle of the submandibular gland fossa. The mean concavity depth on the right side (2.86±0.70 mm) was significantly greater than that on the left side (2.45±0.68 mm). Although the mean distance from the deepest point of the submandibular gland fossa to the alveolar crest along the longitudinal axis of the tooth was smaller on the right side compared to the left side, this difference was not statistically significant (Table 2).

Table 2. Mean concavity angle, depth, and distance from the deepest point of the fossa to the alveolar crest according to side

Variable	Right (n=79) Mean±SD	Left (n=79) Mean±SD	Total Mean±SD	p-value
Angle (degrees)	42.99±7.67	42.53±8.18	42.76±7.91	0.723
Depth (mm)	2.67±0.60	2.45±0.68	2.56±0.65	0.037
Distance (mm)	13.73±2.63	14.20±2.45	13.96±2.36	0.203

Discussion

According to the results of this study, different anatomical factors of the submandibular gland fossa-including the location, depth, concavity angle, and distance from the alveolar crest-differ according to population, sex, and side of the mandible, which necessitate careful evaluation in implant treatment. According to previous studies, deep submandibular fossa in the mandibular molar region is not observed in all individuals. Based on the posterior mandibular ridge morphology classification described by Chan et al. (12), this deep fossa is specific to the U-shaped ridge group. In the present study, which was conducted on an Iranian population, this morphology had the highest frequency (56.4%). The study populations in studies by Parnia et al. (13), Ebrahimnejad et al. (14), and Panjnoush et al. (8) were also Iranian, yet the reported frequencies of U-shaped ridge were 80%, 51%, and 56%, respectively. The finding of Panjnoush et al. (8) was approximately similar to that of the present study, whereas the results of Ebrahimnejad et al. (14) and Parnia et al. (13) differed from our study. In studies from other countries, the frequency of this ridge morphology in the molar region was reported as follows: 32.8% in a Malaysian population by Tan et al. (7); 60% and 66% in the United States by Yoon et al. (15) and Chen et al. (16), respectively; 75-77% in Dutch and Turkish populations by Topbas et al. (17); 72-77% in a Turkish population by Kamburoglu et al. (10); 36-39% in a Japanese population by Watanabe et al. (18); and 38.93% in a Swiss population by Braut et al. (19).

The C-shaped morphology, which had the lowest frequency (10%) in the present study, was the most frequent in the study by Tan et al. (7), observed in 51.7% of that population. The frequency of C-shaped morphology was 49% in the study by Ebrahimnejad et al. (14), 3% in the study by Yoon et al. (15), and 13.6% in the study by Chan et al. (12). Overall, these differences reflect anatomical variations across different populations and ethnicities, underscoring the necessity of population-specific studies.

Preoperative assessment of submandibular gland fossa depth is mandatory prior to implant placement in the posterior mandible, especially when the fossa is deep; unrecognized depth may lead to lingual plate perforation (6). In the present study, this depth was calculated as 2.86±0.70 mm in males and 2.42±0.57 mm in females. These values are greater than those reported by Vhatkar et al. (6) and Koushal et al. (1), who calculated these figures as 1.86 mm and 1.74 mm, and 1.73±0.415 mm and 1.57±0.321 mm in males and females, respectively, and are lower than those reported by Nawwar (11), who calculated 4.85 mm and 4.09 mm in males and females, respectively. Panjnoush et al. (8) reported the overall mean depth (males and females combined) as 2.32±1.36 mm; Kamburoğlu et al. (10) and Chan et al. (12) reported 2.40 mm; and Tan et al. (7) reported 2.0±1.2 mm. The overall mean depth in the present study was 2.56±0.65 mm, which is higher than the aforementioned studies (7, 8, 10) but lower compared to Ebrahimnejad et al. (14) and Parnia et al. (13), who reported 3.22±0.92 mm and 2.6±0.85 mm, respectively. In addition to racial and population differences, these discrepancies may be attributed to variations in the extent of the studied region, dentate or edentulous status of the jaws, and the imaging modality used (CT vs. CBCT).

In the present study, the relationship between sex and concavity depth was statistically significant. This significant association was also observed in studies by Koushal et al. (1), Nawwar (11), and Khodabakhshian et al. (20), but was not significant in studies by Ebrahimnejad et al. (14), Yoon et al. (15), Kamburoğlu et al. (10), Vhatkar et al. (6), and Parnia et al. (13).

In contrast to the study by Koushal et al. (1), the present study also demonstrated a statistically significant relationship between side and concavity depth, with a higher frequency of deep submandibular gland fossa on the right side than on the left. This finding is consistent with the results of Khodabakhshian et al. (20). However, in the study by Nawwar (11), fossa depth was greater on the left side than on the right.

The mean concavity angle of the submandibular gland fossa in the present study was 42.76±7.91 degrees, which is lower than the values reported by Ebrahimnejad et al. (14) (50.42±4.75 degrees), Tan et al. (7) (50.6 degrees), and Chan et al. (12) (57.7 degrees). In the study by Panjnoush et al. (8), the mean concavity angle was 15.45±16.19 degrees, which is substantially lower than both the present study and the other aforementioned studies (7, 12, 14). Beyond racial and anatomical variations, these discrepancies may be attributed to differences in the extent of the ridge region studied and the methodological approaches employed for measurement.

Another factor influencing implant size selection and placement is alveolar bone height (6, 14), which in the present study was measured as the distance from the deepest point of the submandibular gland fossa to the alveolar crest. This height was significantly greater in males (15.34±2.31 mm) compared to females (13.33±2.10 mm), and the difference was statistically significant. The overall mean height in the present study was 13.96±2.36 mm, which is lower than the values reported by Vhatkar et al. (6) (14.1450 mm) and Tan et al. (7) (15.3±3.2 mm). The measurement method used in the present study was more similar to that of Vhatkar et al. (6), and the obtained values showed smaller discrepancies. Nevertheless, racial and anatomical variations across different populations remain the primary explanation for differences in measurements.

Specifically, the use of cross-sectional buccolingual images allows for more precise presurgical implant planning, and the American Academy of Oral and Maxillofacial Radiology considers their use essential in this context. To achieve this, the most advanced imaging modality introduced is cone-beam computed tomography (CBCT), which generally offers lower radiation dose and cost compared to CT while providing clear three-dimensional information (10, 13). This contributes significantly to improved treatment quality by creating a more predictable postoperative implant position (6). All studies reviewed in this investigation, with the exception of Parnia et al. (13) (which used CT), employed this modality.

In the present study, the location of the deepest point of the submandibular gland fossa was also investigated. To the best of our knowledge, no previous study has examined the location of the deepest fossa point with this level of precision. In the present investigation, all cases were dentate in both molar regions, and unlike other studies (8, 10-12, 14, 15, 17), the present study was conducted precisely on normal population anatomy rather than on populations that had experienced bone resorption and morphological changes following tooth loss over time. The location of the deepest fossa point was determined by examining CBCT cross-sectional images on the right and left sides, as well as in females and males. This point was located more posteriorly in males, most frequently corresponding to the distal half of the mandibular second molar, whereas in females it was most frequently located at the junction between the mandibular first and second molars. This difference was statistically significant. In the studies by Tan et al. (7) and Nawwar (11), the deep submandibular gland fossa was generally reported to occur most frequently adjacent to the second molar. In the present study, the location of the deepest point differed between the right and left sides; however, this difference was not statistically significant.

The results of this study demonstrated that the frequency of deep submandibular gland fossa is relatively high, observed in 56.4% of the population. The location of the deepest point, depth, concavity angle, and distance to the alveolar crest-all presented in this study-provide useful information for surgeons and dentists when planning implant treatment in the mandibular first and second molar regions.

Given the high prevalence of deep submandibular gland fossa in the studied population, thorough pre-implant evaluation of this region using CBCT is essential prior to implant therapy in the mandibular molar areas.

Acknowledgment

We hereby express our gratitude to the Vice-Chancellor for Research and Technology of Shahid Sadoughi University of Medical Sciences, Yazd, for supporting this study. We also extend our thanks to the esteemed professors and members of the Department of Radiology, School of Dentistry, Shahid Sadoughi University of Medical Sciences, Yazd, for their cooperation in conducting this research.

References

1.Koushal D, Tangotra A. Evaluation of the depth of submandibular gland fossa and its correlation with mandibular canal in vertical and horizontal locations using CBCT. Int J Radiol Diagn Imaging. 2022;5(4):04-11.
2.Camargo IB, Van Sickels JE. Surgical complications after implant placement. Dent Clin North Am. 2015;59(1):57-72.
3.Saad I, Salem S. Knowledge, awareness, and perception of dental students, interns, and freshly graduated dentists regarding dental implant complications in Saudi Arabia: a web-based anonymous survey. BMC oral Health. 2021;21(1):161.
4.Resnik R. Misch's Contemporary Implant Dentistry, 4th ed. Elsevier Health Sciences; 2020.
5.Nilsun B, Canan B, Evren H, Kaan O. Cone-Beam Computed Tomography Evaluation of the Submandibular Fossa in a Group of Dental Implant Patients. Implant Dent. 2019;28(4):329-39.
6.Vhatkar BS, Shetty NK, Waghmare MS, Pagare SS, Vahanwala SP, Santosh V. Submandibular gland fossa assessment with cone beam computed tomography. Int J Sci Stud. 2019;7(4):53-7.
7.Tan WY, Ng JZL, Ajit Bapat R, Vijaykumar Chaubal T, Kishor Kanneppedy S. Evaluation of anatomic variations of mandibular lingual concavities from cone beam computed tomography scans in a Malaysian population. J Prosthet Dent. 2021;125(5):766.e1-8.
8.Panjnoush M, Eil N, Kheirandish Y, Mofidi N, Shamshiri AR. Evaluation of the concavity depth and inclination in jaws using CBCT. Caspian J Dent Res. 2016;5:17-23. [In Persian]
9.Anbiaee N, Yazdani B. Comparison of the Position and View of the Inferior Alveolar Canal and Mental Foramen in Panoramic Radiography and CBCT Images. J Babol Univ Med Sci. 2022;24(1):413-22. [In Persian]
10.Kamburoğlu K, Acar B, Yüksel S, Paksoy CS. CBCT quantitative evaluation of mandibular lingual concavities in dental implant patients. Surg Radiol Anat. 2015;37(10):1209-15.
11.Nawwar A. Evaluation of lingual concavities in the posterior mandibular area using Cone beam computed tomography scans in an Egyptian population-A cross-sectional study. Egypt Dent J. 2022;68(4):3401-10.
12.Chan HL, Brooks SL, Fu JH, Yeh CY, Rudek I, Wang HL. Cross-sectional analysis of the mandibular lingual concavity using cone beam computed tomography. Clin Oral Implants Res. 2011;22(2):201-6.
13.Parnia F, Fard EM, Mahboub F, Hafezeqoran A, Gavgani FE. Tomographic volume evaluation of submandibular fossa in patients requiring dental implants. Oral Surg Oral Med Oral Pathol Oral Radiol Endod. 2010;109(1):e32-6.
14.Ebrahimnejad H, Haghani J, Safaee A, Jahankhah AS, Rad M. Evaluation of Mandibular Lingual Concavity in Premolar and Molar Region Using Cone-Beam Computed Tomography (CBCT). J Kerman Univ Med Sci. 2022;29(1):24-30.
15.Yoon TY, Patel M, Michaud RA, Manibo AM. Cone Beam Computerized Tomography Analysis of the Posterior and Anterior Mandibular Lingual Concavity for Dental Implant Patients. J Oral Implantol. 2017;43(1):12-8.
16.Chen LC, Lundgren T, Hallström H, Cherel F. Comparison of different methods of assessing alveolar ridge dimensions prior to dental implant placement. J Periodontol. 2008;79(3):401-5.
17.Topbas NK, Özemre MÖ, Uzun C, Orhan K, Gülşahı A, Van Der Stelt P, et al. Relationship of the Presence of Lingual Concavity and Mandibular Canal Location: A Retrospective Two-Center Study. Mersin Üniversitesi Tıp Fakültesi Lokman Hekim Tıp Tarihi ve Folklorik Tıp Dergisi. 2022;12(1):170-8.
18.Watanabe H, Mohammad Abdul M, Kurabayashi T, Aoki H. Mandible size and morphology determined with CT on a premise of dental implant operation. Surg Radiol Anat. 2010;32(4):343-9.

19.Braut V, Bornstein MM, Kuchler U, Buser D. Bone dimensions in the posterior mandible: a retrospective radiographic study using cone beam computed tomography. Part 2--analysis of edentulous sites. Int J Periodontics Restorative Dent. 2014;34(5):639-47.
20.Khodabakhshian A, Mollaei M, Alimohammadi M, Ghobadi F, Hosseinnataj A, Gholampour A. Assessing the variations of the depth and angle of the submandibular gland fossa and the mandibular canal using cone beam computed tomography (CBCT): Submandibular gland fossa assessment using CBCT. Regen Reconstr Restor. 2024;9:e4.